



Full Length Article

Burning velocity and Markstein length blending laws for methane/air and hydrogen/air blends



D. Bradley*, M. Lawes, R. Mumby

School of Mechanical Engineering, University of Leeds, Leeds LS2 9JT, UK

ARTICLE INFO

Article history:

Received 3 May 2016

Received in revised form 2 August 2016

Accepted 9 September 2016

Available online 28 September 2016

Keywords:

Laminar burning velocity

Markstein number

Hydrogen/methane blends

Blending laws

ABSTRACT

Because of the contrasting chemical kinetics of methane and hydrogen combustion, the development of blending laws for laminar burning velocity, u_l , and Markstein length for constituent mixtures of CH₄/air and H₂/air presents a formidable challenge. Guidance is sought through a study of analytical expressions for laminar burning velocity. For the prediction of burning velocities of blends, six blending laws were scrutinised. The predictions were compared with the measured burning velocities made by Hu et al. under atmospheric conditions [1]. These covered equivalence ratios ranging from 0.6 to 1.3, and the full fuel range for H₂ addition to CH₄. This enabled assessments to be made of the predictive accuracy of the six laws. The most successful law is one developed in the course of the present study, involving the mass fraction weighting of the product of u_l , density, heat of reaction and specific heat, divided by the thermal conductivity of the mixture. There was less success from attempts to obtain a comparably successful blending law for the flame speed Markstein length, L_b , despite scrutiny of several possibilities. Details are given of two possible approaches, one based on the fractional mole concentration of the deficient reactant. A satisfactory empirical law employs mass fraction weighting of the product $u_l L_b$.

© 2016 The Authors. Published by Elsevier Ltd. This is an open access article under the CC BY license (<http://creativecommons.org/licenses/by/4.0/>).

1. Introduction

There is increasing interest in supplementing natural gas supplies with the addition of hydrogen. This has led to a number of experimental and chemical kinetic [1,2] studies of the burning velocities, u_l , of such blends with air. The interest in this extends beyond such practicalities to the general problem of deriving satisfactory blending laws for fuel/air mixtures, with very different burning velocities and chemical kinetics. For example, the laminar burning velocity, u_l , of a stoichiometric mixture at 303 K and 0.1 MPa of CH₄ is 0.35 m/s, whereas that for H₂/air is 2.05 m/s. This large difference makes the prediction of CH₄/H₂ burning velocities a particularly challenging test for blending laws.

One of the approaches adopted is based on earlier analytical derivations of expressions for the laminar burning velocity, involving profiles of volumetric heat release rates. An important difference in flame structure between CH₄/air and H₂/air flames is revealed by the profiles of the volumetric heat release rates, normalised by their maximum values, q/q_{\max} , and plotted against the reaction progress variable, c . Values of such profiles computed from earlier detailed chemical kinetics studies [3] are shown in

Fig. 1 by the two contrasting dotted curves. The full line curve is a more approximate algebraic fit. The maximum heat release rate of the faster burning H₂ mixture occurs at a distinctively lower value of c . This is a consequence of enhanced molecular transport and low temperature reaction, both attributable to H atoms, with a resulting increase in u_l . The kinetic modeling in [2] shows how the blend u_l of CH₄/H₂ flames increases with the concentration of H. Exceptionally, in hydrogen flames, such is the upstream diffusion of H atoms and the consequent induced reactivity, the concept of a flame thickness based on an inert preheat zone is of limited validity [4]. The contrasting aspects of CH₄ and H₂ flame structures make the development of accurate blending laws for u_l values of their blends more exacting than the development of such laws for hydrocarbon blends.

The present paper explores the application of six different laws, for predicting the burning velocities of blends of CH₄/air and H₂/air, at the same equivalence ratio, ϕ . One of the laws is entirely new and was developed in the course of the present study. Probably the earliest blending law was that of Le Châtelier [5] for predicting the lean flammability limit of a blend, based upon the reciprocal of mole fraction weighting of those of the constituent fuels. A common approach is to employ a property of the constituent mixtures, all at the same ϕ , designated by i and j for a binary blend, with an appropriate quantitative weighting of that property. Frequently

* Corresponding author.

E-mail address: d.bradley@leeds.ac.uk (D. Bradley).

Nomenclature

a	air mole/fuel mole	T_{ai}	activation temperature, based on $u_i \rho_u$ (K)
a_s	stoichiometric air mole/fuel mole	\tilde{T}_a	activation temperature based on u_i (K)
c	reaction progress variable	T_u	unburned temperature (K)
c_p	mean specific heat at constant pressure (J/mass/K)	T_b	burned temperature (K)
h	sensible enthalpy (J/mol)	u_l	unstretched laminar burning velocity (m/s)
h_f	enthalpy of formation (J/mol)	\bar{x}	mixture mole fraction
k_u	mixture thermal conductivity (J/m/K/s)	\bar{x}_f	fuel mole fraction
k_m	mean thermal conductivity (J/m/K/s)	\bar{x}_i	i 'th constituent mole fraction
L_b	burned gas Markstein length (m)	x	mass fraction
Le	Lewis number	x_f	fuel mass fraction
Ma_b	burned gas Markstein number	x_i	i 'th constituent mass fraction
\bar{m}_i	species i mole fraction	\bar{x}_d	deficient reactant mole fraction
\bar{m}_R	reactant mole fraction	Z	Zel'dovich number = $(T_a/T_b^2)(T_b - T_u)$
P	pressure (Pa)		
q	heat release rate (J/s)		
q_{\max}	maximum volumetric heat release rate (J/m ³ s)		
\bar{Q}	molar heat of reaction (J/mol)		
Q	mass heat of reaction (J/kg)		
$R(c)$	heat release rate source term (J/m ³ s)		
r	laminar flame radius (m)		
S_n	stretched flame speed (m/s)		
S_s	unstretched flame speed (m/s)		
t	time (s)		
T	temperature (K)		

Greek symbols

α	flame stretch rate (1/s)
δ	flame thickness (m)
λ	burning velocity eigenvalue
ν	kinematic viscosity (m ² /s)
ρ_u	unburned mixture density (kg/m ³)
ρ_b	burned mixture density (kg/m ³)
ϕ	equivalence ratio

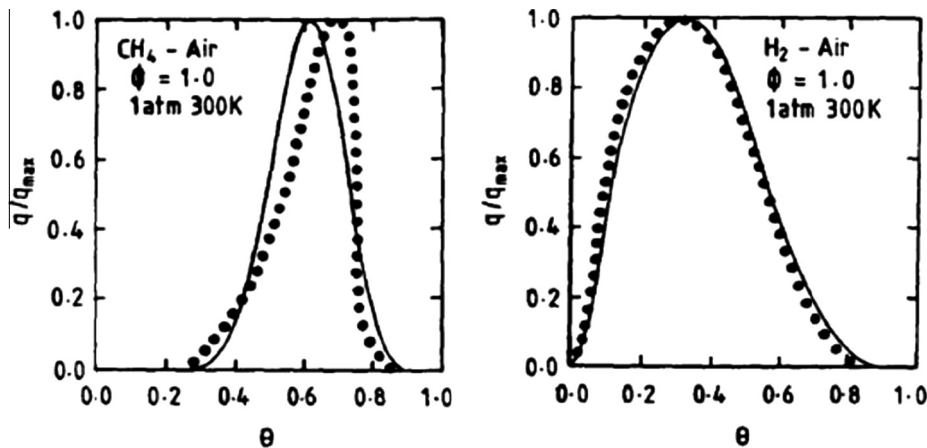


Fig. 1. Dotted curves show volumetric heat release rate profiles from detailed chemical kinetics, for CH₄/air and H₂/air mixtures from [3]. θ is the reaction progress variable, c . The full line curve is a more approximate algebraic fit.

the property employed is the laminar burning velocity of the constituent mixtures, u_{li} , along with mole or mass fractional weightings, \bar{x}_i , or, x_i , respectively, of the constituent mixtures. The burning velocity of the blend, u_{lb} , expressed in terms of the fractional mass concentrations of the constituent fuel/air mixtures, x_i and x_j and their respective burning velocities is:

$$u_{lb} = x_i u_{li} + x_j u_{lj}. \quad (1)$$

The expression for fractional mole weighting, indicated by \bar{x}_i is similar.

Burning velocities also are affected by the flame stretch rate and, for this, a convenient and relevant parameter is the Markstein length, L_b . This can be derived directly from flame speed measurements in spherical explosions, as in [1]. The chemical kinetic computational studies in [6] show how Markstein lengths can be

derived from these, that are associated, with the laminar burning velocity and the separate effects of both strain rate and flame curvature. This is applied to experimentally measured values in [7]. Normalised by the laminar flame thickness these give the corresponding Markstein numbers. In contrast to u_l , no blending laws are known to the authors for L_b .

Two possible approaches for Markstein length blending laws are considered. One is based on weighting the value of L_b for each constituent mixture by the fractional mole concentration of the deficient reactant (fuel or oxygen). The other, involves fractional mole concentration weighting of the product $u_l L_b$ for each constituent mixture.

The different blending laws for u_l and L_b are first formulated and discussed. Each is then employed to predict the values of these parameters for blends of CH₄/air and H₂/air at the same ϕ , over

the same ranges of measurement of spherical explosions as were employed in the experiments in [1]. These cover the full range of CH₄/H₂ ratios and a wide range of ϕ values. The ratio of predicted to measured values are then compared over these wide ranges, for the different blending laws.

2. Mixture compositions

Before introducing possible blending laws, it is first necessary to define how the various constituent mixtures, their blends, and their proportions of fuel, are specified. This requires the composition of constituent mixtures to be expressed in terms of the value of ϕ . For one mole of fuel and a moles of air:

$$\phi = (1/a)(1/a_s)^{-1}, \quad (2)$$

where $_s$ indicates the moles of air for one mole of fuel in a stoichiometric mixture.

One mole of constituent fuel/air mixture is comprised of:

$$\left[\frac{1}{1 + (1/\phi)(1/a_s)^{-1}} \right] \text{ mole of fuel and } \left[\frac{(1/\phi)(1/a_s)^{-1}}{1 + (1/\phi)(1/a_s)^{-1}} \right] \text{ mole of air.} \quad (3)$$

This simplifies to:

$$\left[\frac{\phi}{\phi + a_s} \right] \text{ mole fuel} + \left[\frac{a_s}{\phi + a_s} \right] \text{ mole air.} \quad (4)$$

Now consider a binary blend of two constituent fuel/air mixtures, one with fuel i , the other with fuel j , both with the same ϕ . Let the blend consist of a mole fraction \bar{x}_i of the first constituent mixture and of \bar{x}_j of the second mixture. Note $\bar{x}_i + \bar{x}_j = 1$. The composition of one mole of the blend is:

$$\left[\frac{\phi}{\phi + a_{si}} \right] \bar{x}_i \text{ moles fuel } i + \left[\frac{\phi}{\phi + a_{sj}} \right] \bar{x}_j \text{ moles of fuel } j + \left[\frac{a_{si}}{\phi + a_{si}} \right] \bar{x}_i + \left[\frac{a_{sj}}{\phi + a_{sj}} \right] \bar{x}_j \text{ mole of air.} \quad (5)$$

In general, different fuels, i or j , will have different stoichiometric air requirements and this is signified by the appropriate fuel symbol following a_s . In the present study, for one mole of fuel, $a_{sH_2} = 2.38$ and $a_{sCH_4} = 9.52$.

The mole fraction of fuel i within the total fuels of $(i + j)$ is:

$$\bar{x}_{fi} = \left[\frac{\phi}{\phi + a_{si}} \right] \bar{x}_i \left\{ \left[\frac{\phi}{\phi + a_{si}} \right] \bar{x}_i + \left[\frac{\phi}{\phi + a_{sj}} \right] \bar{x}_j \right\}^{-1}. \quad (6)$$

Fractional mass weightings are obtained from mole fractions by multiplying mass by the appropriate molecular weights, and normalising.

3. The blending laws

3.1. Analytical expressions for burning velocity

A theoretical background is provided for some of the blending laws, not so much by detailed chemical kinetics, as by Spalding's seminal mathematical analyses of the laminar burning velocity [8–10]. His expression for the mass burning rate flux $u_l \rho_u$, for a Lewis number of unity, is:

$$u_l \rho_u = \left[\frac{k_u \int_0^1 R(c) dc}{\lambda (T_b - T_u) c_p^2} \right]^{0.5}. \quad (7)$$

Here k_u is the thermal conductivity of unburned gas, T_u , the initial temperature, c_p , the mean specific heat, and ρ_u the density of unburned gas. The integral is that of the volumetric heat release

rate source term, $R(c) = (k/k_u)H\dot{m}$, in which H is the mass-based heat of reaction of the fuel, and \dot{m} its mass volumetric rate of burning, with respect to the reaction progress variable, c , given by the fractional temperature rise, $(T - T_u)/(T_b - T_u)$. The numerical value of λ , the burning velocity eigenvalue, was related by Spalding, in an algebraic expression, to the value of c at the centroid of a plot of the heat release rate profile, against c , as in Fig. 1. In terms of Eq. (7), as the maximum of the heat release rate profile moves to lower values of c , λ decreases with the centroid distance, and u_l consequently increases.

Eq. (7) can be expressed as

$$(Qc_p/k_u)^{0.5} u_l \rho_u = \left[\frac{\int_0^1 R(c) dc}{\lambda} \right]^{0.5}, \quad (8)$$

with Q the heat of reaction of unit mass of the mixture. Computations in [3] show that higher values of Q and u_l are associated with smaller values of λ . The numerator within the larger brackets represents a volumetric heat release rate integrated in c space. This, with Q , exerts the dominant influence on u_l .

If $S(c)$ represents the product of reactant concentrations, Arrhenius "A" values, k/k_u , heat of reaction, any effect of non-unity Lewis number, Le , and the activation temperature for the heat release rate, T_a , then:

$$\int_0^1 R(c) dc = \int_0^1 S(c) \exp(-T_a/T) dc. \quad (9)$$

Because $dc/dT = (T_b - T_u)^{-1}$, it can be shown:

$$\int_0^1 R(c) dc = \int_0^1 S(c) \left[\frac{T_a}{T^2} (T_b - T_u) \right]^{-1} d \exp(-T_a/T). \quad (10)$$

The high activation energy, asymptotic, assumption [11], that all the heat release occurs at T_b , results in a value of λ of 0.5 and a single valued volumetric heat release rate, q_{\max} , at $c = 1$. Eq. (10) then becomes:

$$\int_0^1 R(c) dc = \int_0^1 S(1) \left[\frac{T_a}{T_b^2} (T_b - T_u) \right]^{-1} \exp(-T_a/T_b) = (S(1)/Z) \exp(-T_a/T_b), \quad (11)$$

in which Z is the Zel'dovich number, $= (T_a/T_b^2)(T_b - T_u)$.

Eq. (7) then becomes

$$u_l \rho_u = \left[\frac{k_m S(1) \exp(-T_a/T_b)}{0.5Z(T_b - T_u)c_p^2} \right]^{1/2}. \quad (12)$$

$$u_l \rho_u = \exp(-T_a/2T_b) \exp \ln \left(\frac{k_m S(1)}{0.5Z(T_b - T_u)c_p^2} \right)^{1/2}, \text{ and} \quad (13)$$

$$u_l \rho_u = \exp \left[(T_a/2T_b) - \ln \left(\frac{k_m S(1)}{0.5Z(T_b - T_u)c_p^2} \right)^{1/2} \right]. \quad (14)$$

If $T_{al} = T_a - 2T_b \ln \left(\frac{k_m S(1)}{0.5Z(T_b - T_u)c_p^2} \right)^{1/2}$, then

$$\frac{T_{al}}{2T_b} = \frac{T_a}{2T_b} - \ln \left(\frac{k_m S(1)}{0.5Z(T_b - T_u)c_p^2} \right)^{1/2}, \text{ and} \quad (15)$$

$$u_l \rho_u = \exp(-T_{al}/2T_b). \quad (16)$$

Here T_{al} is an activation temperature for the laminar burning mass flux, which is dependent upon pressure, P , Lewis number, Le , and $(T_b - T_u)$. It follows from Eq. (16) that

$$2 \ln u_i \rho_u = -T_{al}/T_b, \quad \text{and} \quad \frac{d^2 \ln u_i \rho_u}{d1/T_b} = -T_{al}. \quad (17)$$

This is a frequently used expression in asymptotic analyses [12,7]. Hirasawa et al. [13] employed a slightly different activation temperature, \tilde{T}_a , based on u_i alone rather than $u_i \rho_u$, with:

$$u_i = \exp(-\tilde{T}_a/T_b), \quad \text{or} \quad \ln u_i = -\tilde{T}_a/T_b. \quad (18)$$

3.2. Blending laws for u_i

The six different blending laws for burning velocity that were scrutinised are summarised and referenced in Table 1. Laws 1 and 2 involve fractional mass [14,15] and mole [16] weightings of u_i , as already discussed.

The third law is more complex and is based on the further development by Di Sarli and Di Benedetto [2] of Le Châtelier's original blending law. With \bar{x}_{fi} , the mole fraction of fuel i in all the fuels, in a binary mixture,

$$u_{lb} = [\bar{x}_{fi}/u_{li} + \bar{x}_{fj}/u_{lj}]^{-1}, \quad \text{with} \quad \bar{x}_{fi} + \bar{x}_{fj} = 1. \quad (19)$$

Law 4 is based on the observation in [3] that the burning velocities of lean fuel/air mixtures, within a given chemical family of fuels, increase linearly with the heat of reaction of one mole of the mixture, \bar{Q} . This is found from:

$$\bar{Q} = \sum_P \bar{m}_P (h_f - \Delta h) - \sum_R \bar{m}_R (h_f - \Delta h), \quad (20)$$

where the summation subscripts R and P refer to reactants and products, \bar{m} indicates a species mole fraction, h_f is the enthalpy of formation at the standard state conditions of 298 K and 0.1 MPa, and Δh is the sensible enthalpy. Equilibrium products of combustion at constant pressure and T_b , h_f and Δh were found from the GasEq code [17]. Because of the large chemical differences between H_2 and CH_4 , a blending law for their mixtures, based on such an assumed linearity, is unlikely to be successful.

Law 5 is based on Spalding's expression for the mass rate of burning, in the form of Eq. (8), with mass weighting, x_i and x_j of the integrated reaction rate terms of the constituent fuel/air mixtures:

$$\begin{aligned} \left[(Qc_p/k_u)^{0.5} u_i \rho_u \right]_b &= \left[\int_0^1 \frac{R(c)dc}{\lambda} \right]_b^{0.5} \\ &= x_i \left[\int_0^1 \frac{R(c)dc}{\lambda_i} \right]_i^{0.5} + x_j \left[\int_0^1 \frac{R(c)dc}{\lambda_j} \right]_j^{0.5}. \end{aligned} \quad (21)$$

Alternatively, from Eqs. (8) and (21) applying the fractional mass weighting to the separate $\left[(Qc_p/k_u)^{0.5} u_i \rho_u \right]$, constituent mixture terms gives:

$$(Qc_p/k_u)_b^{0.5} u_{lb} \rho_{ub} = x_i (Qc_p/k_u)_i^{0.5} u_{li} \rho_{ui} + x_j (Qc_p/k_u)_j^{0.5} u_{lj} \rho_{uj}. \quad (22)$$

This new law has two merits, that are particularly relevant to CH_4 /air and H_2 /air blends. First, it is related to the all-important profiles of heat release rate for the constituent mixtures, assumed to be additive, and, second, it invokes the separate thermal conductivities of the two mixtures, which are significantly different. That of H_2 /air, is more than twice that of CH_4 /air, see Fig. 2.

The basis of the sixth law is Eq. (18), from [13]. This is a less direct blending law, in that it is based on blended values of \tilde{T}_a . Values of u_i and T_b are known for each of the constituent mixtures, enabling the respective values of \tilde{T}_a to be found. These are weighted by their respective mole fractions for each constituent mixture to give \tilde{T}_{ab} for the blend, from which u_{lb} can be found, by an inverse process, from Eq. (18).

3.3. Blending laws for L_b

Finding effective blending laws for L_b proved to be more difficult. A number of parametric groupings and weightings were explored. Only the two most satisfactory are presented. The first law, \bar{x}_{di} , was suggested by the role of the Lewis number, based on the deficient reactant, in determining the Markstein number. It involves weighting the L_b value for each constituent mixture by the mole fraction, \bar{x}_{di} , of the deficient reactant:

$$L_{bb} = \bar{x}_{di} L_{bi} + \bar{x}_{dj} L_{bj}. \quad (23)$$

For example, under lean conditions, for the measured L_{bi} , the deficient reactant mole fraction for weighting the constituent mixture i , is the mole fraction of fuel i , expressed as a fraction of the two constituent mixture fuel moles and given by \bar{x}_{fi} in Eq. (6). Here, $\bar{x}_{di} = \bar{x}_{fi}$. Under rich conditions, the deficient reactant mole fraction for mixture i is the mole fraction of oxygen \bar{x}_{oi} expressed as a fraction of the two constituent mixture oxygen moles, given within Eq. (5). Hence:

$$\bar{x}_{di} = 0.21 \left[\frac{a_{si}}{\phi + a_{si}} \right] \bar{x}_i \left\{ 0.21 \left[\frac{a_{si}}{\phi + a_{si}} \right] \bar{x}_i + 0.21 \left[\frac{a_{sj}}{\phi + a_{sj}} \right] \bar{x}_j \right\}^{-1}. \quad (24)$$

The second law, involves the product, $u_i L_b$, for each constituent mixture, fractional mass weightings, and is more empirical. It takes the form:

$$u_{lb} L_{bb} = x_i u_{li} L_{bi} + x_j u_{lj} L_{bj}. \quad (25)$$

4. Comparisons of measured and predicted values

Predicted values of u_i and L_b for blends of CH_4 /air and H_2 /air at the same ϕ are compared with the experimentally measured values of u_i and L_b of Hu et al. [1], derived from spherical explosions, at 303 K and 0.1 MPa in a cylindrical explosion chamber of 180 mm diameter. Values of ϕ ranged between 0.6 and 1.3, with \bar{x}_{f,H_2} varying between 0 and 1.0. Predicted and experimental values of u_i and L_b values under lean conditions, for $\phi = 0.6$ and 0.8, are shown in

Table 1
Summary of u_i blending laws investigated.

	u_i blending law	Ref.	Symbol	u_p/u_i	σ
1	Fractional mass weighting of u_i of constituent mixtures. Eq. (1)	[14]	x	1.09	0.06
2	Fractional mole weighting of u_i of constituent mixtures. Eq. (1) modified	[16]	\bar{x}	1.2	0.09
3	Modified Le Châtelier law. Fractional mole weighting of constituent fuels. Eq. (19)	[2]	LC	0.92	0.04
4	u_i plotted against \bar{Q} per mole of constituent mixture. Eq. (20)	[3]	\bar{Q}	1.18	0.08
5	Fractional mass weighting of constituent mixture $u_i \rho_u$ with $(Qc_p/k_u)^{0.5}$. Eq. (22)	Present work	Q/k	1.01	0.03
6	Fractional mole weighting of \tilde{T}_a to obtain blend \tilde{T}_a . Eq. (18)	[13]	\tilde{T}_a	0.89	0.04

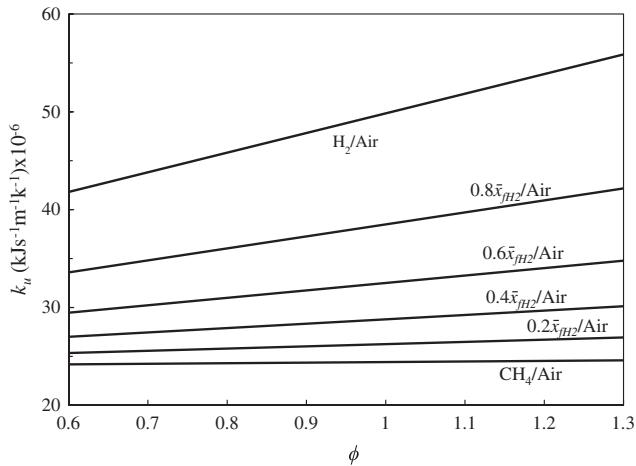


Fig. 2. Variation of thermal conductivity, k_u , with ϕ for methane/air, hydrogen/air, and their blends. $T_u = 303$ K, $P_i = 0.1$ MPa. Values from [17].

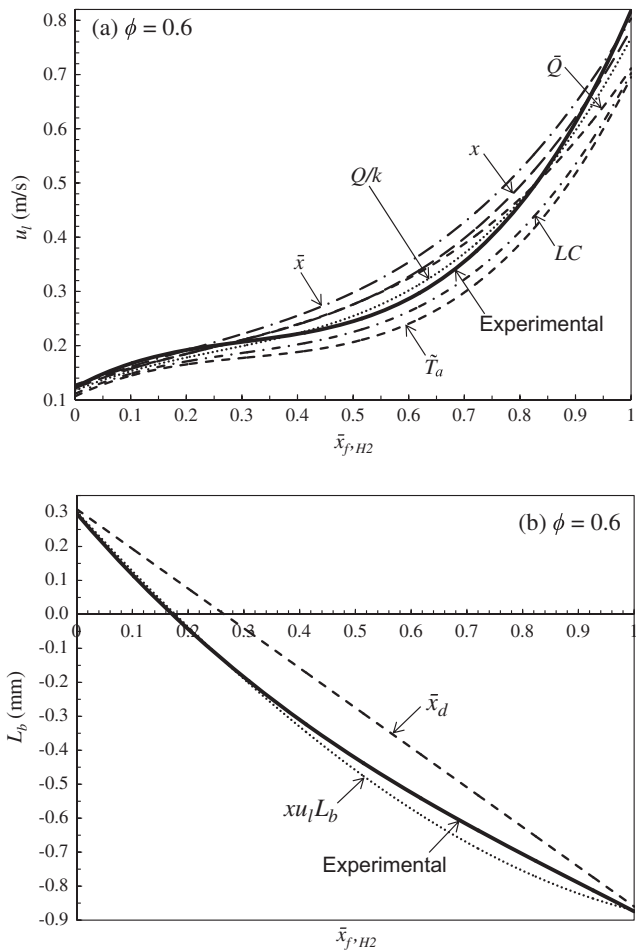


Fig. 3. Predicted and measured values of (a) u_l and (b) L_b for $\text{CH}_4/\text{H}_2/\text{air}$ mixtures, as a function of \bar{x}_{f,H_2} , $\phi = 0.6$. Broken, best fit, curves denote predicted values for each law, full line curves denote experimental values measured by Hu et al. [1].

Figs. 3 and 4, and under stoichiometric and rich conditions, for $\phi = 1.0$ and 1.2, are shown in Figs. 5 and 6.

Measurements of flame speeds were made at flame radii greater than 5 mm, to avoid the influence of ignition energy, and less than 25 mm [1] to avoid cellular flames [18]. There was a linear correlation between flame speed and flame stretch rate [1]. Flame speeds

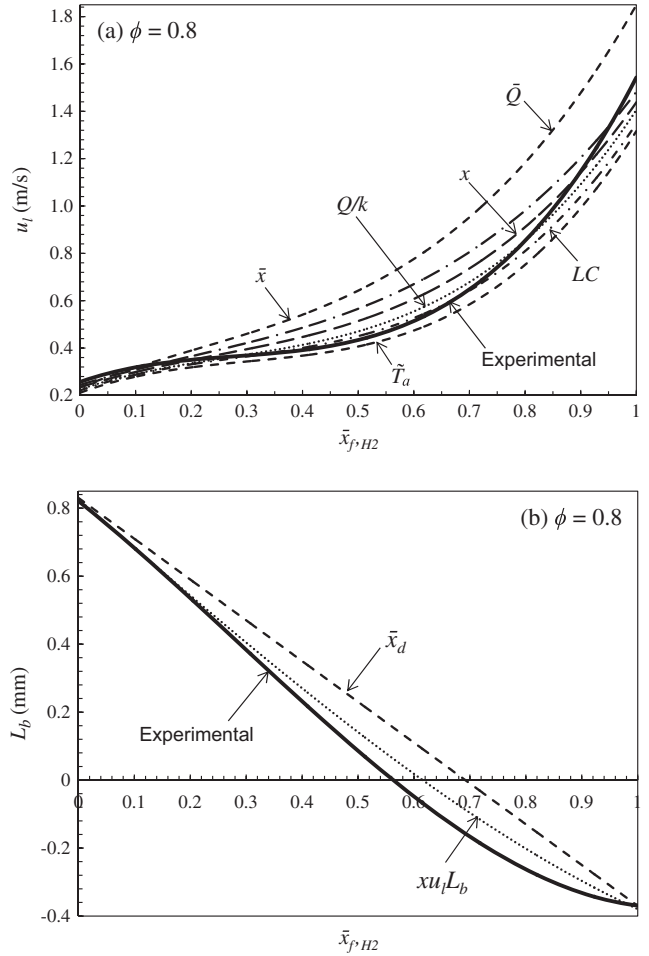


Fig. 4. Predicted and measured values of (a) u_l and (b) L_b for $\text{CH}_4/\text{H}_2/\text{air}$ mixtures, as a function of \bar{x}_{f,H_2} , $\phi = 0.8$. Broken, best fit, curves denote predicted values for each law, full line curves denote experimental values measured by Hu et al. [1].

were extrapolated to zero stretch rate and divided by ρ_u/ρ_b to yield u_l . Interestingly, such flame speeds would, in fact, be unstable and cellular. Critical Karlovitz stretch factors have been obtained, below which flames become unstable. The more negative the Markstein number, the higher the stretch factor required to maintain its stability [19].

Measured values of u_l and L_b , with maximum standard errors of 8.6% and 16.6%, respectively, are shown by the solid curves, while the predicted values are shown by symbols in Table 1 for each of the various blending laws for u_l .

Tables 2 and 3 summarise the ratios of predicted to measured burning velocities, u_{lp}/u_l , for the different blending laws, for $\phi = 0.6$ and 0.8 and $\phi = 1.0$ and 1.2, as a function of \bar{x}_{f,H_2} . Likewise, Table 4 summarises the ratio of predicted to measured Markstein lengths, L_{bp}/L_b for the different blending laws, for $\phi = 0.6$ –1.2, also as a function of \bar{x}_{f,H_2} . For each table, at the bottom of each column, a value of the ratio, averaged over all values of \bar{x}_{f,H_2} , is given for the given law and value of ϕ . Below these values are the corresponding standard deviations, σ .

5. Discussion

5.1. Blending laws for u_l

The final two columns in Table 1 give the overall values of u_{lp}/u_l , averaged over all values of \bar{x}_{f,H_2} and ϕ , ranging from 0.6 to 1.3, with

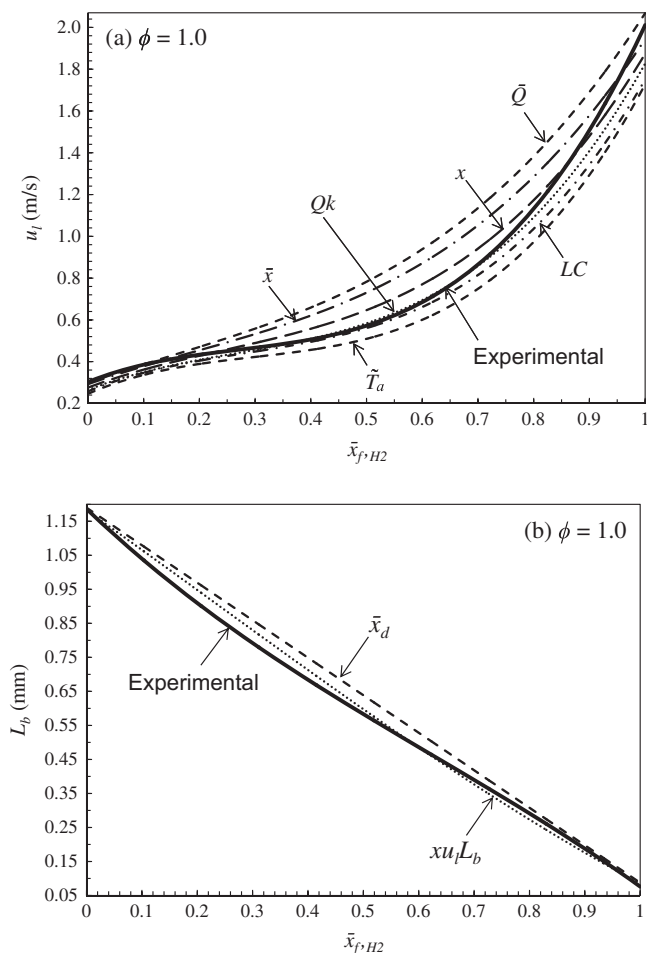


Fig. 5. Predicted and measured values of (a) u_l and (b) L_b for $\text{CH}_4/\text{H}_2/\text{air}$ mixtures, as a function of \bar{x}_{f,H_2} , $\phi = 1.0$. Broken, best fit, curves denote predicted values for each law, full line curves denote experimental values measured by Hu et al. [1].

their overall standard deviation, σ of such values. The best predictions are those of the Q/k law. Importantly, this is the only law that gives predictions which are within the 8.6% accuracy of measurement of u_l . This is not surprising, because it involves more parameters, Eq. (22) is based on the mass fraction weighting of constituent mixture heat release rates, specific heats, and the values of k . An empirical improvement in the law's accuracy of prediction occurred when Q was replaced by the molar \bar{Q} . This reduced the overall average value of u_{lp}/u_l from 1.05 to 1.01 and decreased σ to 0.04. The second best law is that involving mass weighting. This gives predictions, some of which have errors that exceed 10%.

The worst predictions were those from the \bar{x} and \bar{Q} laws. Expectations for the \bar{Q} law were bound to be low. Fig. 2 in [3] demonstrates the consequences of the two fuels belonging to quite different chemical families. Only for $\phi = 0.6$ is this law satisfactory. It is rather more surprising that the fractional mole, \bar{x} , law was so unsatisfactory and inferior to fractional mass weighting. Both of these laws consistently over-estimated u_l .

Equally consistently, the \tilde{T}_a law under-estimated values of u_l . This was based on fractional mole weighting. Fractional mass weighting gave even more pronounced underestimations for this law. In contrast, the LC , modified Le Châtelier law, which was formulated specifically for CH_4/H_2 blends [2], both under and over-estimated u_l . This was the only law based on the fraction of fuel, rather than of mixture. All the laws became unsatisfactory for ϕ

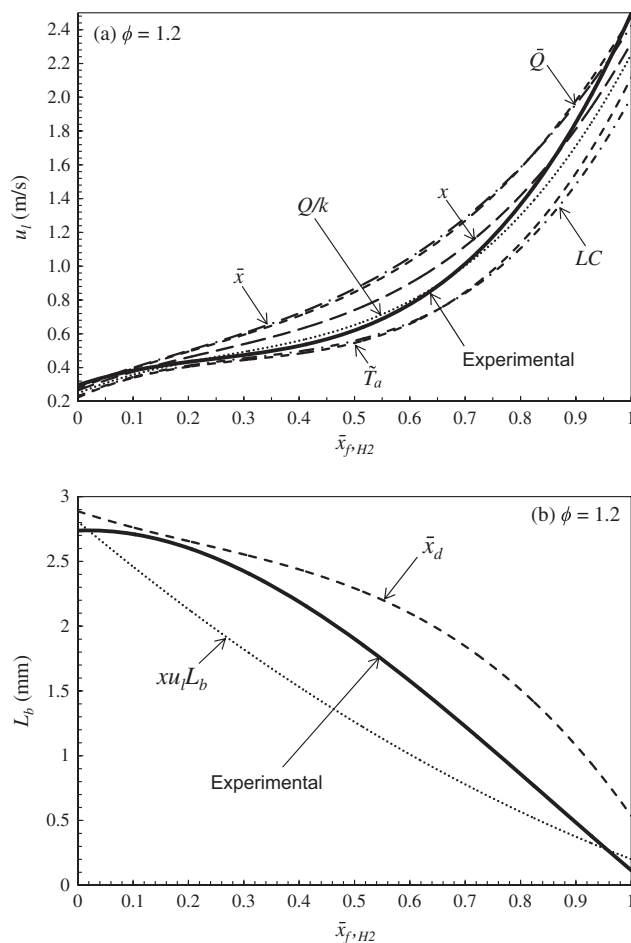


Fig. 6. Predicted and measured values of (a) u_l and (b) L_b for $\text{CH}_4/\text{H}_2/\text{air}$ mixtures, as a function of \bar{x}_{f,H_2} , $\phi = 1.2$. Broken, best fit, curves denote predicted values for each law, full line curves denote experimental values measured by Hu et al. [1].

values of 1.3 and higher. It was found that the order of merit of the different laws also applied to their performance, over wide ranges of conditions for diverse hydrocarbon/air mixtures, but these predictions were less challenging than those for the present CH_4/air and H_2/air blends.

5.2. Blending laws for L_b

For the predicted values of L_b , only those predicted by the $xu_l L_b$ law at $\phi = 1.0$ have an accuracy better than the worst measured error of 16.6%. Figs. 4(b) and 5(b) indicate acceptable predictions with this law at $\phi = 0.8$ and 1.0. The predictions at $\phi = 1.2$ in Fig. 6(b) are less acceptable. The \bar{x}_d law consistently over-estimates values, particularly as \bar{x}_{f,H_2} is increased, although its performance is satisfactory up to \bar{x}_{f,H_2} values of 0.2.

5.3. Laminar burn power flux

This is given by the product of mixture density, mass heat of reaction and laminar burning velocity. It is an indicator of the flame power as more H_2 is added to CH_4 . Based on the measured values of u_l , this is shown in kW/m^2 in Fig. 7. As the mole fraction of H_2 is increased, the increased burning velocity of the mixture more than compensates for the lower heat of reaction of hydrogen and the burn power flux increases. The increase is particularly pronounced for \bar{x}_{f,H_2} above 0.5.

Table 2
Ratios of predicted to measured burning velocities, u_{fp}/u_i , for different blending laws, ϕ values of 0.6, and 0.8, as a function of \bar{x}_{f,H_2} . Values of u_i for constituent mixtures: at $\phi = 0.6$, 0.822 m/s and at $\phi = 0.8$, 1.546 m/s for H_2 /air and at $\phi = 0.6$, 0.121 m/s, and at $\phi = 0.8$, 0.27 m/s for CH_4 /air.

\bar{x}_{f,H_2}	\bar{x}		x		LC		\bar{T}_a		\bar{Q}		Q/k	
	$\phi = 0.6$	$\phi = 0.8$										
0.1	1.10	1.03	1.07	1.00	1.02	0.97	0.99	0.94	1.08	1.06	1.05	0.97
0.2	1.09	1.07	1.04	1.02	0.94	0.96	0.90	0.91	1.05	1.13	0.99	0.97
0.3	1.11	1.13	1.05	1.06	0.91	0.97	0.85	0.91	1.05	1.24	0.98	0.99
0.4	1.12	1.20	1.04	1.11	0.87	0.99	0.80	0.92	1.04	1.34	0.96	1.03
0.5	1.13	1.29	1.04	1.18	0.85	1.04	0.78	0.94	1.04	1.46	0.96	1.08
0.6	1.23	1.27	1.14	1.16	0.91	1.01	0.83	0.91	1.12	1.48	1.04	1.06
0.7	1.19	1.30	1.10	1.19	0.88	1.03	0.81	0.94	1.07	1.53	1.02	1.09
0.8	1.18	1.14	1.11	1.06	0.90	0.93	0.84	0.86	1.06	1.38	1.04	0.99
0.9	1.13	1.05	1.08	1.00	0.93	0.91	0.90	0.87	1.00	1.29	1.04	0.96
Av.	1.14	1.16	1.07	1.08	0.91	0.98	0.86	0.91	1.06	1.32	1.01	1.02
σ	0.05	0.11	0.03	0.08	0.05	0.04	0.07	0.03	0.03	0.16	0.03	0.05

Table 3
Ratios of predicted to measured burning velocities, u_{fp}/u_i , for different blending laws, ϕ values of 1.0, and 1.2, as a function of \bar{x}_{f,H_2} . Values of u_i for constituent mixtures at $\phi = 1.0$, 2.05 m/s and at $\phi = 1.2$, 2.51 m/s, for H_2 /air and at $\phi = 1.0$, 0.353 m/s and $\phi = 1.2$, 0.326 m/s for CH_4 /air.

\bar{x}_{f,H_2}	\bar{x}		x		LC		\bar{T}_a		\bar{Q}		Q/k	
	$\phi = 1.0$	$\phi = 1.2$										
0.1	1.04	1.14	1.01	1.08	0.98	1.00	0.96	0.99	1.07	1.12	0.98	1.04
0.2	1.11	1.28	1.04	1.16	0.98	1.02	0.94	1.00	1.15	1.26	0.99	1.08
0.3	1.08	1.23	0.99	1.09	0.91	0.90	0.86	0.88	1.13	1.21	0.93	0.99
0.4	1.17	1.32	1.05	1.15	0.94	0.91	0.88	0.89	1.23	1.30	0.97	1.03
0.5	1.30	1.36	1.16	1.17	1.02	0.90	0.94	0.88	1.38	1.33	1.06	1.04
0.6	1.20	1.27	1.07	1.09	0.93	0.82	0.85	0.81	1.29	1.24	0.97	0.97
0.7	1.27	1.35	1.14	1.17	0.99	0.88	0.91	0.88	1.37	1.33	1.04	1.05
0.8	1.12	1.17	1.02	1.04	0.89	0.80	0.84	0.82	1.20	1.16	0.94	0.95
0.9	1.05	1.06	0.99	0.98	0.91	0.81	0.87	0.85	1.13	1.07	0.95	0.93
Av.	1.15	1.24	1.05	1.10	0.95	0.89	0.89	0.89	1.22	1.23	0.98	1.01
σ	0.09	0.10	0.06	0.07	0.04	0.08	0.04	0.07	0.11	0.09	0.04	0.05

Table 4
Ratios of predicted to measured Markstein lengths, L_{fp}/L_b , for different blending laws, with ϕ values of 0.6–1.2, as a function of \bar{x}_{f,H_2} . Values of L_b , for constituents mixtures at $\phi = 0.6$, –0.86 mm, at $\phi = 0.8$, –0.37 mm, $\phi = 1.0$, 0.087 mm and at $\phi = 1.2$, 0.2106 mm for H_2 /air and at $\phi = 0.6$, 0.31 mm, at $\phi = 0.8$, 0.83 mm, at $\phi = 1.0$, 1.19 mm, at $\phi = 1.2$, 2.81 mm for CH_4 /air.

\bar{x}_{f,H_2}	\bar{x}_d				xuL_b			
	0.6	0.8	1.0	1.2	0.6	0.8	1.0	1.2
0.2	–0.95	1.18	1.07	1.10	0.46	1.09	1.05	0.88
0.4	0.54	1.21	1.13	1.09	1.14	0.93	1.08	0.68
0.6	0.80	–1.22	0.98	1.13	1.17	–0.20	0.90	0.54
0.8	0.83	0.52	1.23	2.75	1.01	0.81	1.09	1.03
Av.	0.31	0.42	1.10	1.52	0.94	0.66	1.03	0.79
σ	0.85	1.14	0.11	0.82	0.33	0.58	0.09	0.22

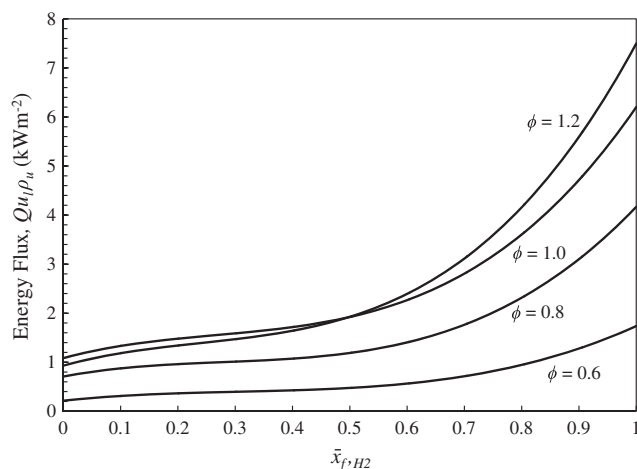


Fig. 7. Energy flux variation as a function of \bar{x}_{f,H_2} , for $\phi = 0.6, 0.8, 1.0$ and 1.2 .

6. Conclusions

Six blending laws for laminar burning velocity have been tested as predictors for CH_4 /air and H_2 /air blends over a wide range. Because of their different chemical kinetics and burning velocities, such blends provide a good test of the suitability of the different blending laws. Their performances, in descending order of merit, for each weighting law, are Q/k, mass, mole, \bar{T}_a , mixture mole \bar{Q} , and mole. The Q/k law also has the best theoretical basis, through its heat release rate/reaction progress variable profile. Quite empirically, it is improved when \bar{Q} is substituted for Q. Interestingly, as the proportion of H_2 increases, the heating flux of a laminar flame sharply increases, as the effect of increasing burning velocity dominates over that of decreasing heat of reaction. This first attempt to find an accurate blending law for the Markstein length proved to be more difficult, but two were suggested. One of the problems is the rather wide error bands for the measured values. Further chemical kinetic studies of both strained and curved flames would improve understanding in this area.

Acknowledgements

Erjiang Hu, Zuohua Huang, Jiajia He, Chun Jin and Jianjun Zheng are thanked for collaboration and for kindly providing additional u_l and L_b data. Thanks are expressed to EPSRC for the award of a Research Scholarship to R.M.

References

- [1] Hu Erjiang, Huang Zuohua, He Jiajia, Jin Chun, Zheng Jianjun. Experimental and numerical study on laminar burning characteristics of premixed methane–hydrogen–air flames. *Int J Hydrogen Energy* 2009;34:4876–88.
- [2] Di Sarli V, Di Benedetto A. Laminar burning velocity of hydrogen–methane/air premixed flames. *Int J Hydrogen Energy* 2007;32:637–46.
- [3] Bradley D, Habik SE-D, El-Sherif SA. A generalisation of laminar burning velocities and volumetric heat release rates. *Combust Flame* 1991;87:336–45.
- [4] Göttgens J, Mauss F, Peters N. Analytic approximations of burning velocities and flame thicknesses of lean hydrogen, methane, ethylene, ethane, acetylene and propane flames. *Proc Combust Inst* 1992;24:129–35.
- [5] Le Châtelier H. Estimation of firedamp by flammability limits. *Ann Mines* 1891;19(8):388–95.
- [6] Bradley D, Gaskell PH, Gu XJ. Burning velocities, Markstein lengths, and flame quenching for spherical methane–air flames: a computational study. *Combust Flame* 1996;104:176–98.
- [7] Bradley D, Hicks RA, Lawes M, Sheppard CGW, Woolley R. The measurement of laminar burning velocities and Markstein numbers for iso-octane–air and iso-octane–n-heptane–air mixtures at elevated temperatures and pressures in an explosion bomb. *Combust Flame* 1998;115:126–44.
- [8] Spalding DB. Mixing rule for laminar flame speed. *Fuel* 1956;35:347–51.
- [9] Spalding DB. Predicting the laminar flame speed in gases with temperature-explicit reaction rates. *Combust Flame* 1957;1:287–95.
- [10] Spalding II DB. One-dimensional laminar flame theory for temperature-explicit reaction rates. *Combust Flame* 1957;1:296–307.
- [11] Zel'dovich YaB, Frank-Kamenetskii DA. A theory of thermal propagation of flame. *Zh Fiz Khim* 1938;12:100–5.
- [12] Peters N, Williams FA. The asymptotic structure of stoichiometric methane/air flames. *Combust Flame* 1987;68:185–207.
- [13] Hirasawa T, Sung CJ, Joshi A, Yang Z, Wang H, Law CK. Determination of laminar flame speeds using digital particle image velocimetry: binary fuel blends of ethylene, n-butane, and toluene. *Proc Combust Inst* 2002;29:1427–34.
- [14] van Lipzig JPJ, Nilsson EJK, de Goey LPH, Konnov AA. Laminar burning velocities of n-heptane, iso-octane, ethanol and their binary and tertiary mixtures. *Fuel* 2011;90:2773–81.
- [15] Yumlu VS. The effects of additives on the burning velocities of flames and their possible prediction by a mixing rule. *Combust Flame* 1968;12:14–8.
- [16] Payman W, Wheeler RV. The composition of gaseous fuels in relation to their utilisation. *Fuel Sci Practice* 1922;1:185–96.
- [17] Morley C. GasEq: a chemical equilibrium program for windows; 2005. <<http://www.gaseq.co.uk>>.
- [18] Bradley D, Lawes M, Kexin Liu, Verhelst S, Woolley R. Laminar burning velocities of lean hydrogen–air mixtures at pressures up to 1.0 MPa. *Combust Flame* 2007;149:162–72.
- [19] Bradley D, Lawes M, Mansour MS. Explosion bomb measurements of ethanol–air laminar gaseous flame characteristics at pressures up to 1.4 MPa. *Combust Flame* 2009;2009(156):1462–70.